공학석사 학위논문

Investigation of the mechanism of $SrRuO_3/SrTiO_3$ bipolar resistive switching device by transmission electron microscopy

투과전자현미경을 이용한 $SrRuO_3/SrTiO_3$ 양극성 저항변화 소자의 메커니즘 규명

2015 년 8 월

서 울 대 학 교 대 학 원

재 료 공 학 부

조 해 림

Abstract

Investigation of the mechanism of $SrRuO_3/SrTiO_3$ bipolar resistive switching device by transmission electron microscopy

Haelim Cho

Department of Materials Science and Engineering

College of Engineering

Seoul National University

Nowadays, as Information technology (IT) makes rapid advance and the contemporary memory devices have reached its limit in application, high potential memory devices are needed which are not based on the existed memory device's way. Therefore, a number of more powerful and functional nonvolatile memory (NVM) have been extensively explored, and resistive random access memory (ReRAM) device is becoming one of the candidates which displays distinct advantages such as fast switching speed, large resistance ratio, low riving voltage and simple structure.

ReRAM is based on the “resistive switching” (RS) phenomenon, of which the resistance of the metal-insulator-metal (MIM) structured device could be repeatedly set to different resistance by external electric field and these resistance states are corresponding to the binary data storage of 0 and 1. ReRAM can be clarified into two categories by resistive switching behavior, unipolar resistive switching which resistance depends only on magnitude of voltage and bipolar resistive switching which resistance is only depends on the polarity of voltage. In unipolar mode, the mechanism of the resistive switching has been already researched enough and it was revealed that formation and rupture of conductive path, filament, in insulating thin film is the origin of resistive switching phenomenon. However, in case of bipolar mode, there are lots of models which explain the resistive switching. One of them is the formation and rupture of the filament as well as unipolar switching. Many researchers have been proposed for homogeneous bipolar resistive switching by the change at the interface state. In this mechanism, microstructure of interface is the most important factor to determine the resistance change, however, there are not enough experimental evidences for microstructural change directly.

Here, we investigated the $SrRuO_3$ and $SrTiO_3$ single crystal junction device as the most ideal system for investigation of homogeneous

bipolar resistive switching model for TEM experiment. We confirmed the resistive switching and electrical property by I-V curve and did TEM, STEM-EELS analysis to observe the microscopic mechanism. Beside, by using the *In-situ* STM/TEM holder, we observed the operation of the device and the microscopic change simultaneously. The variation of oxygen vacancy concentration at the interface which has been used for explaining the homogeneous bipolar resistive switching was not detected by electron energy loss spectrum in this experiment. Therefore, these results mean that there is another possibility of determining the resistive switching or the amount of oxygen vacancies is too small to detect in well-defined interface. Finally, the finding may be of help to know about the homogeneous bipolar resistive switching mechanism.

Keywords: ReRAM, bipolar resistive switching, $SrTiO_3$, $SrRuO_3$, transmission electron microscopy, and electron-energy loss spectroscopy

Student Number: 2013-23045

List of Figures

Contents

Chapter 1. Introduction

As modern information technology makes rapid advance, memory device should display characteristics such as high density, low energy operation, low cost, fast writing and erasing time, and high performance with respect to endurance and retention. However, current high density mass memory technologies such as dynamic random access memory devices (DRAM) and Flash are expected to approach their scaling limits in the near future. In order to overcome the problems of contemporary memory device and obtain a more powerful and functional nonvolatile data memory (NVM), a number of alternatives have been extensively explored including ferroelectric random access memory (FeRAM), magnetoresistive RAM (MRAM), phase-change RAM (PRAM), etc. Resistive random access memory (ReRAM) device is one of the candidates for ultimate NVM because of its fast switching speed, low driving voltage, large on/off ratio, and simple structure.

A resistive switching memory cell in a ReRAM is generally composed of a capacitor-like MIM structure, which means an insulating or semiconducting material ‘I’ sandwiched between two metal electrodes ‘M’. The MIM cells are electrically switched between at least two different resistance states when an electrical stimulus is applied and the resistance states are applied as the memory signal. By applying appropriate voltage pulses, a

cell in its high-resistance (OFF) state can be SET to a low-resistance (ON) state or RESET back into the OFF state.

Resistive switching has been commonly observed in various dielectric materials including oxide, chalcogenides, and sulfides. There are many ways to classify the various kinds of ReRAM devices, and generally, it is classified by resistive switching behavior. Both the SET and RESET operation can be achieved by the amplitude of the applied voltage in unipolar resistive switching device. On the other hand, for bipolar resistive switching device, the SET and RESET process is only possible at the opposite bias. Unipolar switching has been widely investigated for a long time, and the mechanism is generally explained by formation and rupture of the conducting filament, however, for bipolar resistive switching, the origin of the resistive switching is still completely unknown. Although the colossal electroresistance effect has been extensively studied, both experimentally and theoretically, the precise mechanism involved is not yet understood.[1]

Here, we report a systematic study of resistive switching of metal/oxide interfaces formed between $SrRuO_3$ and $SrTiO_3$. SRO is known for a highly conducting metal and has a high chemical stability in the absence of chemical substitution, and besides, it has a lattice parameter of 0.3955nm which is well matched with the STO, 0.3905nm. Use of such a well-defined interface may enable us to reveal the intrinsic transport properties of the oxide Schottky junctions. Therefore, the SRO/STO junction is expected to be a

suitable system for elucidating the homogeneous bipolar resistive switching mechanism for TEM experiment.

We confirmed the resistive switching and electrical property by measurement of the current-voltage (I-V) curves. Analytical transmission electron microscopy (TEM, Tecnai F20) including high-resolution image, electron diffraction and scanning transmission electron microscopy (STEM)/electron-energy loss spectroscopy (EELS) were employed to elucidate the change at the interface, and besides, *In-situ* scanning tunneling microscope/transmission electron microscope double tilt holder was additionally employed to probe the I-V measurement for direct observation with cell operating. We conducted an experiment to analyze the electronic structure and distribution of particular atom at the vicinity of the interface depending on the resistance state. The experimental results will be explained by the previous presented mechanism or new mechanisms that can account for the experimental results. Finally, we expect that the mechanism investigation may be useful to know about the resistive switching behavior and apply the cell in the future.

Chapter 2. Literature research

2.1 ReRAM

Electronic memory devices have vast applications in almost every area of modern life. Essentially, all modern electronic devices have memories either embedded or externally attached. In addition, the emerging of the personal electronics such as laptop computers, digital cameras, smart phones, tablets and other entertainment devices in the past two decades has resulted in a dramatic increase in the demand for such memory devices. Consumers' consistent desire to have better and cheaper memory has motivated researchers to pursue the continued advancement of memory technology.

Due to the scaling limitations of current Flash technology, it is desirable to discover new technologies such that the scaling can be continued further. More than that, it is very attractive to find one kind of memory which has the combinational advantages of both SRAM and Flash such that it not only has fast program, erase and access time but also has good non-volatility as well as high density characteristics. This type of memory can be called universal memory or storage class memory.[2] The requirements of such universal memory will be nonvolatile, scalable, fast, low power and inexpensive. People are trying various technologies and developing new physical concepts to make this type of memory possible. One of most promising candidates is the so called resistive random access memory (ReRAM).

2.1.1 ReRAM background

The history of the resistive change effect in ReRAM can be traced back to the 1960s. In 1962, P.H. Nielsen[3] and colleagues first found the resistive switching in an Au/SiO/Au structure. The further suggested that such an element could be used as a memory device which could be accessed nondestructively. Several years later, several researchers also found similar phenomena in an Al/SiO_x/Au system.[4,5] Due to stability problems and the emergence and successful development of Si based memories,[6] the resistive switching memorie never developed until quite recently. In 2002, W.W. Zhyang and colleagues[7] demonstrated a ReRAM device based on PCMO. They first showed that such a device is capable of providing memory characteristics that are potentially more favorable than that of traditional Flash devices. After that, in 2004, Samsung Electronics[8] demonstrated resistive switching behavior in various transition metal oxides (TMO) such as NiO, TiO_2, HfO_2, and ZrO_2. The devices delivered operating voltage below 3V, programming current around 2mA with 10^6 cycles of endurance. Ever since, ReRAM has become one of the hottest research topics in both academia and industry. The main motivation for people to investigate ReRAM is due to its anticipated advantages, which almost cover all the merits of an ideal memory such as large endurance, long retention, fast access speed, low power and most importantly high density.

Fig1. shows the typical structure of a ReRAM device. Generally, the structure is simple and consists of several layers. Two of them are top electrode and bottom electrode with a resistive layer sandwiched in between.

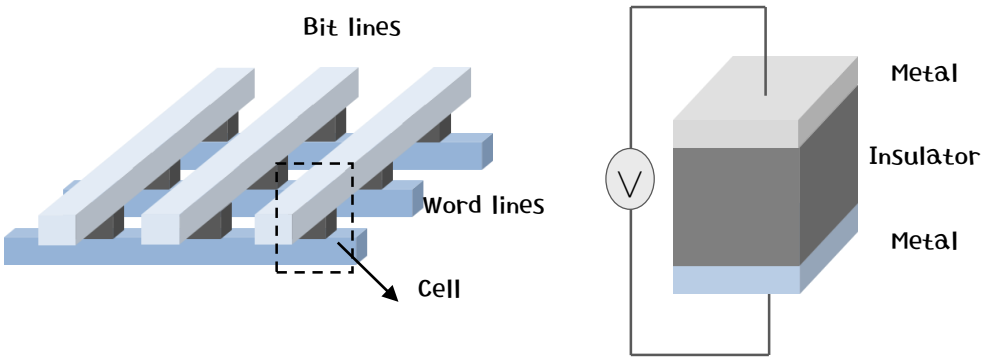

Figure. 1| Typical structure of a ReRAM device.

2.1.2 Classification of ReRAM devices.

There are many ways to classify the various kinds of ReRAM devices. This approach is particularly important and is to classify ReRAM devices based on the symmetry of I-V characteristics during the SET and RESET operation as shown in Fig.2.[9]

Fig. 2(a) illustrates one type of ReRAM device, in which both the SET and RESET operation can be achieved by applying either positive or negative voltage. In other words, there is no polarity dependence of the device I-V characteristics. This type of device is called a unipolar device. It is worthwhile to point out that for such device, the compliance current (CC) has to be applied during the SET operation to avoid excessive heat generation and thus protect the filaments created as part of the SET process. On the other hand, in the RESET process, no CC is applied and a large current is intentionally generated to break the conductive filament and switching the device back to a high resistance state. Thus, for unipolar devices, the RESET current is generally larger than the SET current. Fig. 2(b) demonstrates the other type of ReRAM devices where a stable SET operation is only possible when a positive voltage is applied across the device. On the other hand, the voltage needed for the RESET operation is always opposite to that used in the SET process. In this particular example, the RESET is only achievable when the voltage is negative. This type of device operation mode is called bipolar. The RESET current in bipolar devices is much less than that of unipolar devices, and thus it is more power efficient. Besides, because the V_{SET} and V_{RESET} in bipolar

devices have different polarity, bipolar devices have larger voltage margin, which makes their operation more reliable. The current mainstream technology of ReRAM is based on the bipolar type of devices.

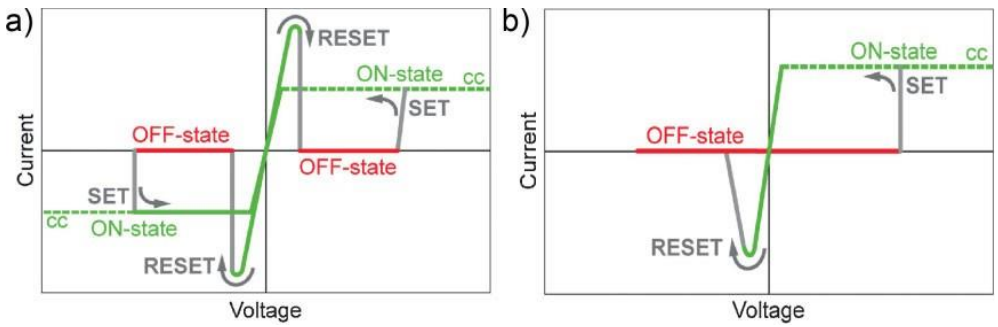

Figure. 2| Two basic operation schemes of resistance switching memory cells. I-V curves recorded for a triangular shaped voltage signal. cc denotes the compliance current. Dashed lines indicate that the real voltage at the system will differ from the control voltage because of the cc in action.

(a) Unipolar switching. The SET voltage is always higher than the RESET voltage, and the RESET current is always higher than the cc during SET operation. (b) Bipolar switching. The SET operation occurs on one polarity of the voltage or current, the RESET operation requires the opposite polarity. In some systems, no cc is used. Please note that the I-V curves of real systems may deviate considerably from these sketches, for both operation schemes.

2.2 Resistive switching mechanism

2.2.1 Unipolar resistive switching mechanism

Unipolar resistive switching mechanism has already been investigated by a number of researchers. Typically, the majority of unipolar mechanisms are explained by conducting filament model and a lot of direct and clear experimental results support this model.

In a filamentary conducting path model, the resistive switching originates from the formation and rupture of conductive filaments in an insulating matrix. The device system which has been mainly researched on is composed of the thin film of a particular material between the two metal electrodes. Binary or ternary transition metal oxides (TMO) such as NiO_2, TiO_2, and SrTiO3 have been widely used for the experiments. In these devices, when given the characteristic voltage walked over to a metal electrode, new secondary conducting phase within the insulating thin film is formed or particular boundaries play a role as a conducting path. With such a phenomenon, the resistance decreases and this is referred to as forming process. In the RESET process, rupture of the filaments takes place and the resistance increases to OFF state back again. In the SET process, opposite to the RESET process, conductive filaments are formed and the resistance decrease again. (Fig.3)[10]

Recent studies suggest that the unipolar resistive switching occurs in the Pt/TiO_2/Pt device and this phenomenon originates from formation and rupture of the filamentary conducting paths in the TiO_2 thin film.[11] In this

system, when a specific voltage was applied, the resistance of the device decreased drastically. The conducting filaments were created between the two metal electrodes and the structure of the filament was identified as the Magneli phase of Ti_4O_7. After switched to the OFF state, this Magneli phase filaments were ruptured, and the filaments were formed again at the ON state. This conducting filament formation phenomenon can be explained by that the oxygen vacancies, already existed in the oxide thin film, are rearranged by the electric field and thermal transport.

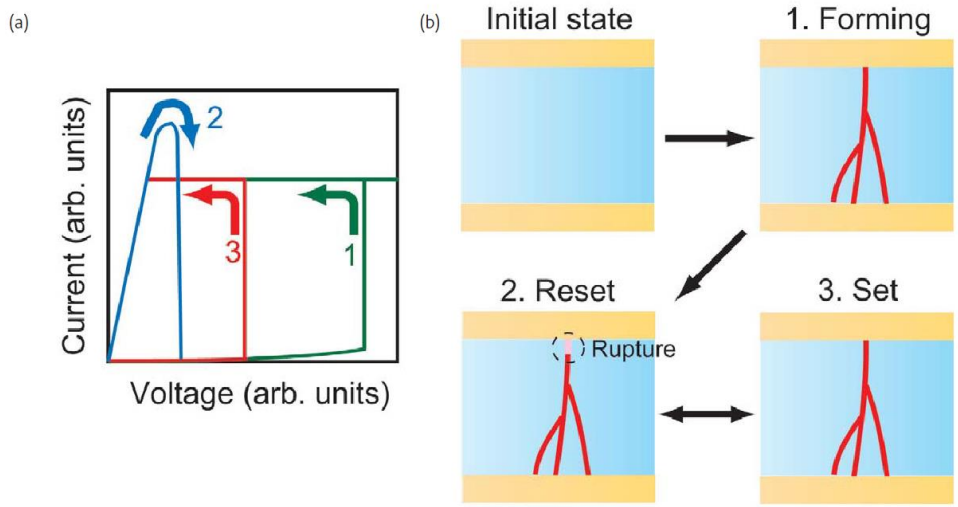

Figure. 3| Unipolar resistive switching behavior. (a) switching I-V curve (b) Schematics of the initial state (as-prepared sample) and (1) forming, (2) reset, and (3) set process.[13]

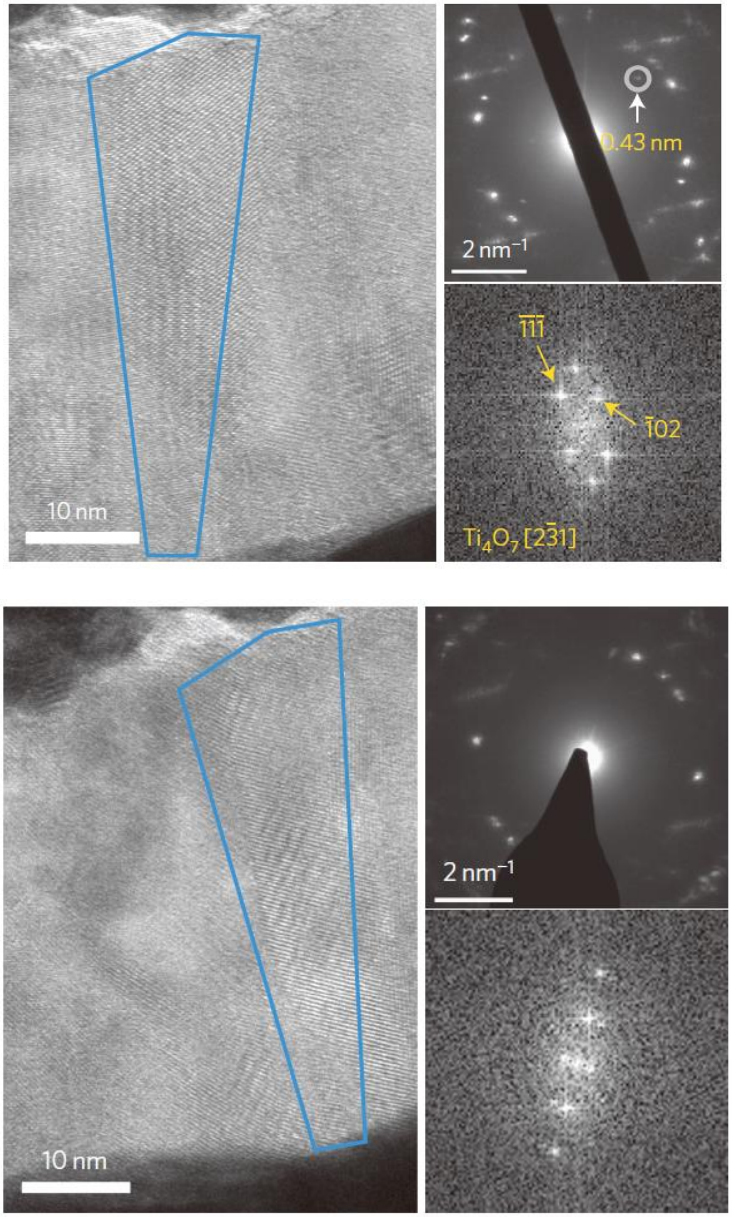

Figure. 4| Conducting filament in TiO_2 thin film (Top) Filament region in OFF state and diffraction pattern of filament structure (Bottom) Filament region in ON state and diffraction pattern of filament structure.

2.1.1. Bipolar resistive switching mechanism

In case of the bipolar resistive switching, it shows a range of the difference according to the electrical characteristics and the material of different systems. Based on the operation principle and device physics, bipolar mechanisms can be classified into two types of devices. One is filamentary type that metal cations of oxygen vacancies make the conducting path, filament, and the other type is the interface type that the change of the interface between metal electrode and insulating matrix induces the resistive switching of the device. For filamentary type, metal cation or oxygen anion is generally diffusive or it easily precipitates such that in the ON state, a conductive metallic bridge is formed. Usually, many groups studying the devices composed of insulating or semiconducting thin film between metal electrodes explain the mechanism for filamentary type. In the metal cation systems, there are activate metal electrode and inert metal electrode. Metal cations from active electrode dissolve into the insulating matrix and move to inert electrode induced by electric field. As a result, at the inert electrode, the cations are reduced and formed as a conducting filament. It is very similar to the unipolar switching mechanism as stated in the previous section. On the other hand, in oxygen anion systems, metal cations are less diffusive or very difficult to precipitate, oxygen anions have a significant role on device performance. Oxygen anion or oxygen vacancies in the insulating matrix move in a certain direction by the electric field and form the conducting bride.

In the interface type, resistive switching takes place at the interface between the metal electrode and the oxide. Usually, this mechanism is used to describe the resistive switching in the contact of transition metal oxide and the metal electrode has a large work function. In this system, the resistance of the device is proportional to the area of the device that can be explained by the filamentary type.[11] However, unlike filamentary type resistive switching devices, the physics of interface type are quite complicated and there are still lots of unknowns. It is considered that there are several types of materials that have these characteristics and even in the same materials, resistive switching properties vary depending on the applied electrical stimulation, and the observation of the microstructure of the interface is relatively difficult. Despite of the vagueness, several basic mechanisms and theories still exist which can at least explain part of the device behavior.

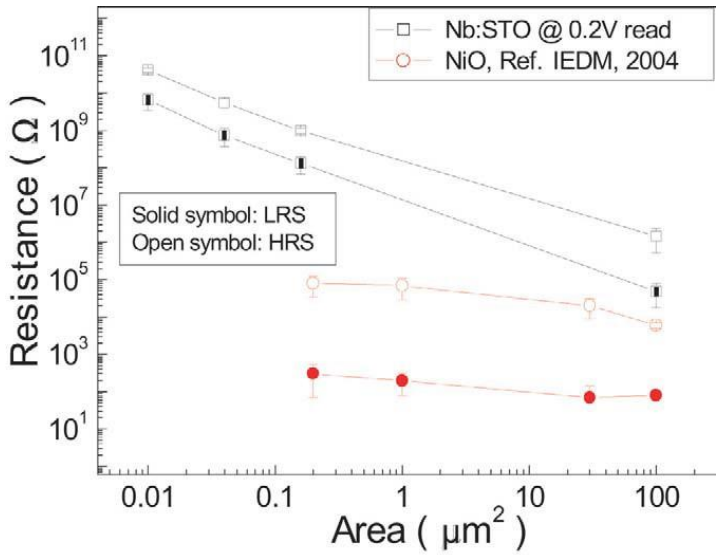

Figure. 5| Area dependence of resistance values in high and low resistance states for Nb-doped $SrTiO_3$ (Nb:STO) and NiO memory cells. The resistance of the Nb:STO memory cells depends linearly on the area, suggesting that the resistive switching takes place over the entire area of the interface. The resistance of NiO memory cells is almost independent of the area, suggesting that resistive switching is a local phenomenon.[12]

(a) electro-chemical migration of ion

One of the mechanisms explaining the interface type resistive switching is that electro-chemical migration of ion induces the resistive switching at the interface on metal/transition metal oxide junctions. A. sawa et al. suggested that oxygen vacancies' movement in the vicinity of the interface brings about the resistance change. Oxygen vacancies are common in transition metal oxide, have a higher mobility than other ions, and besides, oxygen vacancies move directly along the electric field.[14,15] In this paper, the direction of oxygen vacancies' migration is determined by the electric field and the number of oxygen vacancies in the vicinity of the interface may cause the potential barrier to become higher and lower. For example, for SRO/Nb:STO/Ag cells, the as-prepared cells show hysteresis, on the other hand, the annealed sample in an O_2 atmosphere converted into a HRS, and the hysteretic behavior (resistive switching) was suppressed. In the annealing process, the Nb:STO layers are oxidized, i.e. the number of oxygen vacancies in the oxide layers is reduced. Since an oxygen vacancy acts as an effective donor in n-type oxide semiconductors, the reduction in the number of oxygen vacancies may cause the depletion layer to become wider in Nb:STO, resulting in an increase in the contact resistance. Almost full oxidation of the Nb:STO layers may suppress the migration of oxygen vacancies (or oxygen ions), resulting in the suppression of resistive switching. Although these results are not definitive evidence for an electrochemical redox reaction, they do indicate

that the number of oxygen vacancies plays an important role in the change in resistance.

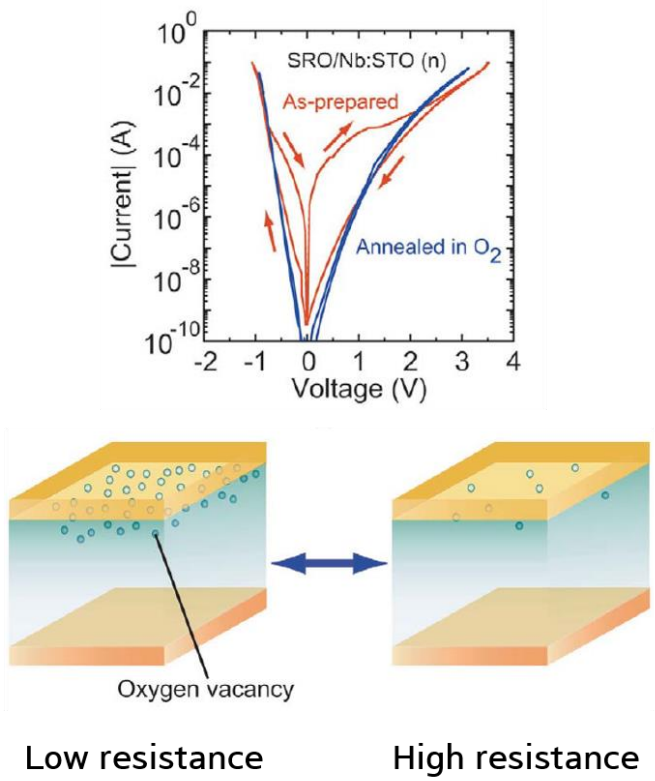

Figure. 6| doping model of bipolar resistive switching mechanism (Top) I-V curve for SRO/Nb:STO/Ag cells. The as-prepared cells show hysteretic I-V characteristics, indicating resistive switching. Annealing under an O_2 atmosphere (oxidative treatment) switches the n-type SRO/Nb:STO/Ag cells into a HRS. (Bottom) Schematics of the changes of the oxygen vacancy density in the vicinity of the interface. The resistance states of the memory cells are possibly determined by the oxygen vacancy density.

There are other studies supporting this mechanism that oxygen vacancies' movement results in the change of the potential barrier height. For instance, one of these studies is direct measurement of the resistance change through simulation. Dmitri B. Strukov et al. demonstrated the change of the potential barrier and resistance change depending on the polarity of the applied voltage through simulating the dynamics of a two-terminal resistive switching device based on a semiconductor thin film with mobile dopants that are partially compensated by a small amount of immobile acceptors. This result is very similar with the experimental results for $Pt/TiO_2/TiO_{2-x}/Pt$ system.[16,17]

To understand the origin of resistive switching definitively, the driving mechanism involved in the switching between two or more resistance states should be elucidated. Recent studies have indicated that the electrochemical migration of oxygen vacancies in the vicinity of the interface drives resistive switching.[18,19]

(b) Fermi level pinning effect by interface states

There is also another mechanism discussed with the movement of the oxygen vacancies.[20] They proposed that the electrical characteristics of the Pt/Nb:STO were determined by interface states. In this system, the rectifying I-V curves indicate the existence of the energy barrier despite high doping concentration of the STO (0.5wt %) enough to show Ohmic behavior.

They employed STEM-EELS analysis to study the interface chemistry. The EELS results clearly showed differences Between HRS and LRS and revealed more oxygen vacancies for the HRS, which is opposed to the generally accepted idea that higher oxygen vacancies at the interface cause LRS in the n-type doped STO. They suggested the mechanism that can describe the experimental results as follows.

If there exist strong interface states, then the energy level of the interface states, instead of the difference between the work function of Pt electrode and conduction band offset of Nb:STO, determines the barrier height. They estimated the potential barrier height by fitting the I-V curves, and these barrier heights are much lower than the theoretical value[21], but closer to the energy difference between conduction band minimum and the interface states introduced by heavy doping.[22] The defect energy levels within the band gap introduced by oxygen vacancies depend on the defect concentration. For the case of STO, the defect level by clustered oxygen vacancies is deeper than that of point oxygen vacancies.[23] The barrier height, determined as the energy difference between conduction band minimum and the interface states,

increases as the interface energy state becomes deeper. This can explain the higher oxygen vacancies in the HRS. As a matter of fact, there have been extensive efforts to explain complex I-V characteristics in real metal-semiconductor interfaces (Ref. R. T. Tung, Appl. Phys. Rev. 1, 011304 (2014) and therein.) and the failure of ideal Schottky barrier model has been ascribed to Fermi level pinning at the interface.

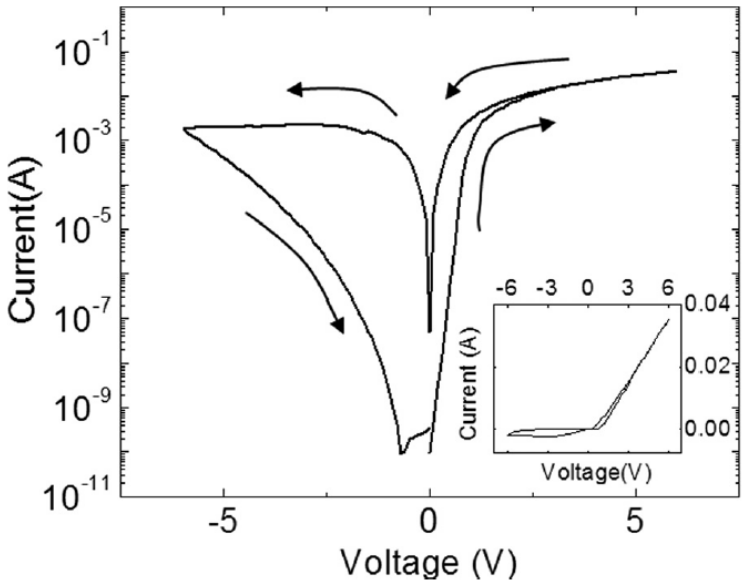

Figure. 7| Current-Voltage (I-V) characteristics curve for Pt/Nb:STO/Ti. It shows that this junction has the rectifying electrical characteristics. Larger variation in resistance switching appears in the negative bias. The linear scale I-V curve (inset) reveals rectifying electrical characteristics.[20]

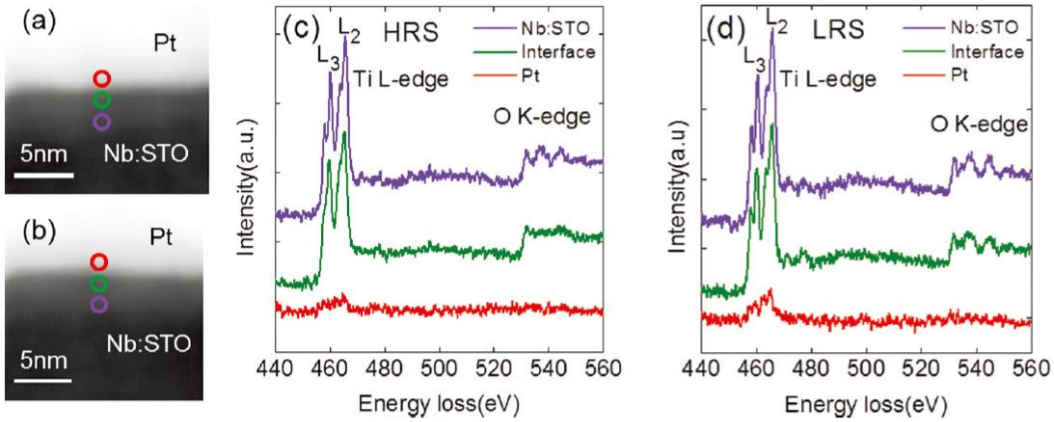

Figure. 8| Annular dark field STEM images of the (a) HRS and (b) LRS sample at the Pt/Nb:STO interface. Energy-loss near-edge structure of the Ti L-edges and O K-edge of the (c) HRS and (d) LRS at the Pt/Nb:STO interface region. The locations in which the spectra are acquired are indicated by circles in the STEM images.[21]

(c) Charge defect trap/de-trap

Charge trapping/de-trapping mechanism is a model of the interface with trapping sites which have sufficiently high density to form a Schottky-like barrier, i.e., the main factor is that the phenomenon occurs at the interface not bulk area.[24] A. Sawa et al. discussed a possible origin of the rectification at the Ti/PCMO interface. Assuming that the Ti/PCMO interface is a Schottky contact, from the I-V characteristics PCMO can be considered as a p-type semiconductor. However, the difference of the interface property between Ag/PCMO and Ti/PCMO cannot be understood by a conventional Schottky contact since Ag and Ti have the almost same work function of ~4.3eV. Thus, an interface-state-induced band bending at the Ti/PCMO interface is considered for the origin of the resistance change. It is well known that when a density of the interface states is high, electronic band in a semiconductor bends at an interface, independently of a work function of an electrode metal.[25]

In this model, the degree of band bending, i.e., barrier width and height, depends on a net charge in the interface states and an energetic distribution of those in the band gap, and this band bending also causes a rectification. Because Ti is a getter for oxygen and has a small electronegativity, the Ti layer possibly extracts a large amount of oxygen atoms from the surface of the PCMO layer. The high density of the interface states induced by the oxygen vacancies may cause a large degree of the band bending at the Ti/PCMO interface, as compared with the Ag/PCMO interface.

On the basis of the interface-state-induced band bending picture, they propose a possible model of the resistance switching. By applying large voltage at the Ti/PCMO interface, a large amount of electrons is accumulated (extracted) into (from) the interface states upon reverse (forward) bias. Accordingly, a variation of a net charge in the interface states leads to a modification of a Schottky-like barrier width and/or height, because the degree of the band bending depends on a net charge in the interface states.

D. J. Seong et al. supports this mechanism that resistance switching can be explained by Schottky barrier modulation in interface traps.[19] If positive bias is applied on the Pt top electrode, electrons are extracted from the interface. The net plus charge make the band width/height narrower/lower, which makes LRS. In contrast, by applying negative bias on the Pt top electrode, a large amount of electrons are accumulated into the interface states, which modifies the bandwidth and barrier height, which in turn, form HRS. This mechanism can be supported by this investigation that an increase in oxygen vacancies resulting from high-pressure hydrogen annealing treatment on Pt/Nb:STO leads to enhancement of the switching behavior.

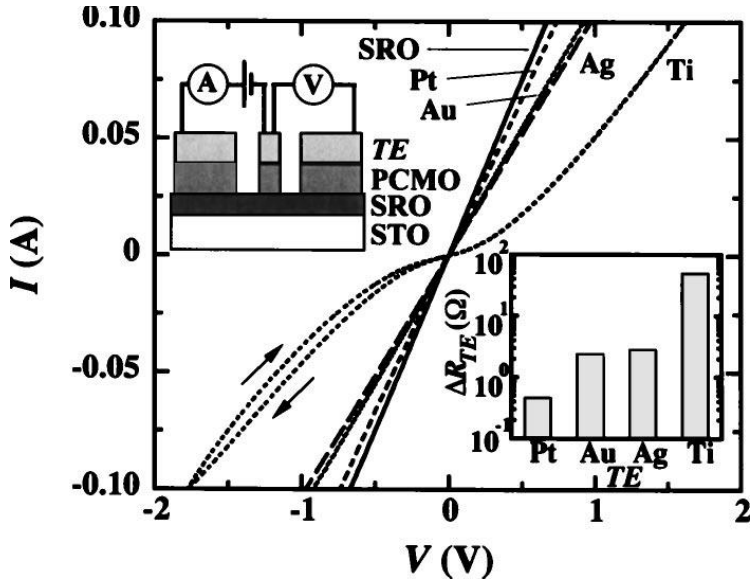

Figure. 9| I-V characteristics of TE/PCMO/SRO layered structures with five different TEs. Here, TE, PCMO, and SRO stand for top electrode, $Pr_{0.7}Ca_{0.3}MnO_3$, and $SrRuO_3$, respectively. The upper panel of the insets shows a schematic of the samples. The lower one shows $\triangle R_{TE}$ ($=R_{TE}-R_{SRO}$) for TE=Pt, Au, Ag, and Ti.

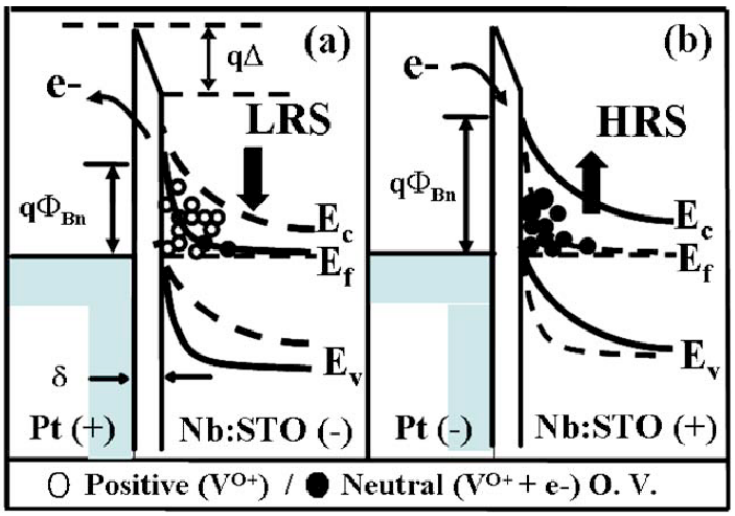

Figure. 10| (a) Potential barrier lowered by charge detrap from the oxygen vacancies. (b) Potential barrier increased by trap at the oxygen vacancies.

(d) Tunneling path

There is another mechanism that explains the resistance switching by trap/detrap at the defect sites. This mechanism assumes that tunneling between the metal electrode and STO causes the major conduction. Also the enhancement or reduction of the resistance switching behavior depends on the doping concentration since the tunneling current determines the resistive switching.[1] In SRO/Nb:STO junctions, no hysteretic behavior was observed in the C-V characteristics, unlike in the I-V characteristics. This suggests that the potential profile of the Schottky barrier remains almost unchanged between the HRS and LRS. In the Schottky barrier, there exist trapping states, such as impurity states and defects. When a large forward bias voltage is applied to the Schottky junction, electrons are discharged from the trapping states, resulting in unoccupied trapping states in the Schottky barrier. In the lower-bias voltage region, electrons can resonantly tunnel through the Schottky barrier using these unoccupied trapping states. When a large reverse-bias voltage is applied, electrons are captured in the trapping states, resulting in the closure of the resonant tunneling paths.

To examine this assumption, another experiment was investigated. The doping level at the interface was intentionally changed, that is, interface-engineered SRO/ X (2nm) / Nb:STO junctions, where X is either undoped STO or very heavily electron-doped $La_{0.25}Sr_{0.75}TiO_3$. As shown in Fig. 11, the SRO/STO/Nb:STO junction remains, showing a rectifying I-V characteristics,

but the hysteretic behavior, i.e. the resistive switching, disappears. This suggests that the 2-nm-thick STO layer prevents the formation of the resonant tunneling paths. Because there is no dopant in the STO layer, there are very few impurity states which host the resonant tunneling. On the other hand, SRO/La:STO/Nb:STO junction shows a quasi-Ohmic behavior and no resistive switching. Because the SRO/La:STO/Nb:STO can be regarded as a metal / n+ / n junction, the Schottky barrier width in the vicinity of the interface is reduced. Thus, electrons possibly pass through the thin Schottky barrier via a direct tunneling process. These results suggest that the presence of the CER effect requires an appropriate doping level which can provide an adequate density of impurity states and thickness of the Schottky barrier for resonant tunneling.

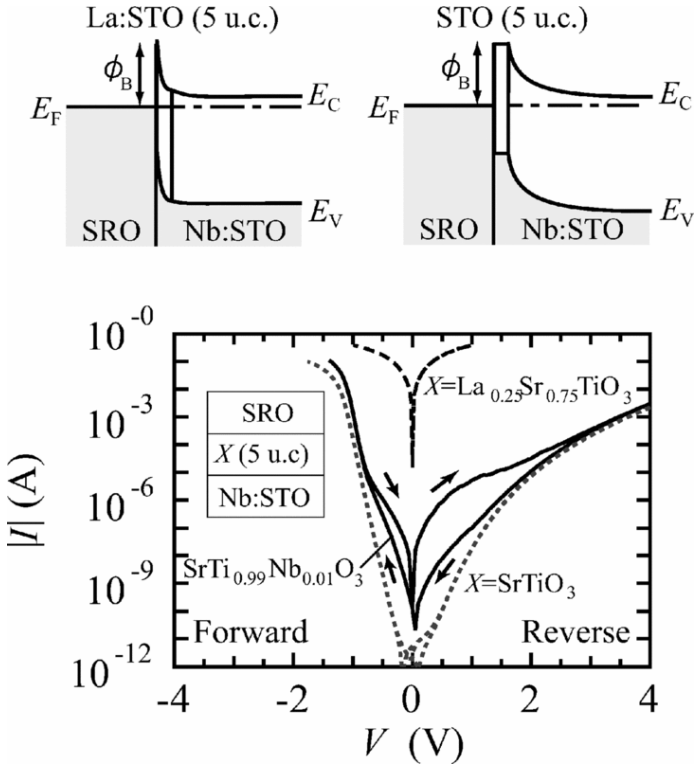

Figure. 11| I-V characteristics of the interface-engineered $SrRuO_3$/ X (2nm) / $SrTi_{1-x}Nb_xO_3$ (x = 0.01) junctions, where X = pristine $SrTiO_3$ (a band insulator) and $Sr_{0.75}La_{0.25}TiO_3$, a metal whose carrier number is much larger than Nb:STO.[26] The CER effect is completely absent in these interface-engineered junctions.

(e) Oxygen vacancy-deficient region effect

Oxygen vacancy-deficient region is also important factor to determine the resistance state for ReRAM devices. In particular device which has a different switching curve direction with general direction, the existence of oxygen vacancy underneath the electrodes is important factor as follows.[13]

When oxygen vacancies are attracted to the interface and are concentrated highly near the interface, the other region becomes oxygen vacancy-deficient. Then, the oxygen vacancy deficient region becomes more electronically resistive. When oxygen vacancy increasingly migrate to the interface, the width of the oxygen vacancy deficient region is widened, causing the overall cell resistance to rise to the HRS. As shown in Figs. , when the oxygen deficient region is widened (narrowed), the electronic barrier for the oxygen vacancy deficient region is raised (lowered), and widened (narrowed); thus, overall, the sample becomes more electronically resistive (conducting).

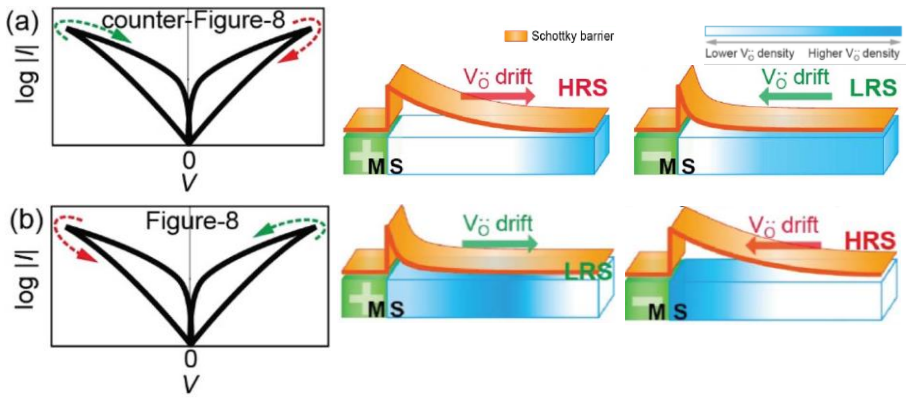

Figure 12| I-V curve and schematics of the resistance switching for each model.[13]

2.3. Structure and electrical characteristics of $SrTiO_3$

Transition metal oxides with the perovskite structure have been widely investigated for the variety of their interesting and intriguing physical properties from both the theoretical and the application point of view. With a perspective toward functional devices, much effort has been put into the study of heterojunctions of these materials. Recent examples include junctions which incorporate ferroelectricity, resistive switching, photo-carrier injection, and magnetic field sensitivity. A common need in all cases is a quantitative understanding of the electronic structure at the interface. In particular, the most fundamental characteristic of rectifying metal-semiconductor junctions is the Schottky barrier height (SBH), which is the energy discontinuity between the Fermi level of the metal and the conduction band minimum (valence band maximum) of the n-type (p-type) semiconductor. Although the SBH can be estimated from current-voltage (I-V) and capacitance-voltage (C-V) measurement, these measures have significant uncertainty arising from limited understanding of the dominant transport mechanisms, as well as unusual features arising from incorporating materials with strongly correlated electrons and nonlinear permittivity.

$SrTiO_3$, one of the typical transition metal oxide with perovskite structure, is relatively stable and is used as an excellent substrate for epitaxial growth of many oxide-based thin films. Its bulk lattice parameter of 3.905Å makes it suitable as the substrate for the growth of many other oxides having

the perovskite structure. $SrTiO_3$ has an indirect band gap of 3.24eV and a direct gap of 3.75eV.[27] Doping strontium titanate with niobium makes it electrically conductive, being one of the only conductive commercially available single crystal substrates for the growth of perovskite oxides.

In the idealized cubic unit cell of such a compound, 'Sr' atom sits at cube corner position, 'Ti' atom sits at body centred position and 'O' atoms sits at face centred positions. However, oxygen vacancies are fairly common in $SrTiO_3$ crystals and thin films even at the room temperature and atmospheric pressure. Oxygen vacancies induce free electrons in the conduction band of the material, making it more conductive and opaque.

$$O_o^x \rightarrow V_o'' + 2e' + \frac{1}{2}O_2$$

$$2Ti_{Ti}^x + 2e' \rightarrow 2Ti_{Ti}'$$

As two electrons pass through the neutral oxygen atom, oxygen vacancies induce free electrons in the conduction band of the materials and cause change in the valence state from Ti^{4+} to Ti^{3+} by the coupling between oxygen vacancies and Ti. Therefore, oxygen vacancies play major roles in electrical and many other properties commonly in oxides. Junctions with Nb-doped $SrTiO_3$ (Nb:$SrTiO_3$), a heavily utilized n-type semiconductor in transition metal oxide heterojunctions, since the permittivity of $SrTiO_3$ varies dramatically at high electric fields.

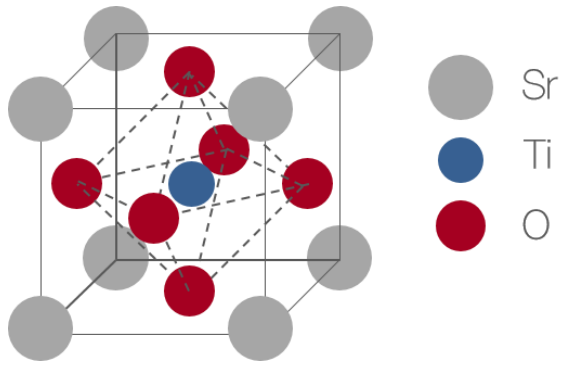

Figure. 13| Schematic of perovskite structure of $SrTiO_3$. The red spheres are oxygen, blue are Ti^{4+} cations, and the grey ones are Sr^{2+}.

3. Experimental method

3.1. Fabrication of the device

3.1.1. Single crystalline bipolar (SRO/STO)

Single crystalline SRO of 50nm thin film was grown by pulsed laser deposition on (001) STO single-crystal substrate. Subsequently, STO of 50nm thin film was grown on SRO by the same process. SRO is known for a highly conducting metal and has a high chemical stability in the absence of chemical substitution, and besides, it has an lattice parameter of 0.3955nm which is close to the STO, 0.3905nm.[28] Furthermore, the interface between SRO and STO is free from a polar discontinuity which can be a significant source of interface states.[29] The SRO surface exhibited a step-and terrace structure as confirmed by atomic force microscopy (AFM) and x-ray diffraction (XRD). (Fig.13-14)

The SRO/STO junction is expected to be a suitable system for elucidating the mechanism of the resistive switching because the SRO film can be epitaxially grown on an STO lattice, resulting in a well-defined interface.[29] Use of such a well-defined interface may enable us to reveal the intrinsic transport properties of the oxide Schottky junctions. The relationship between the resistive switching behavior and the electronic structure at the interface can be elucidated through systematic experimental studies on the junctions, such as the doping level dependence of the transport properties.

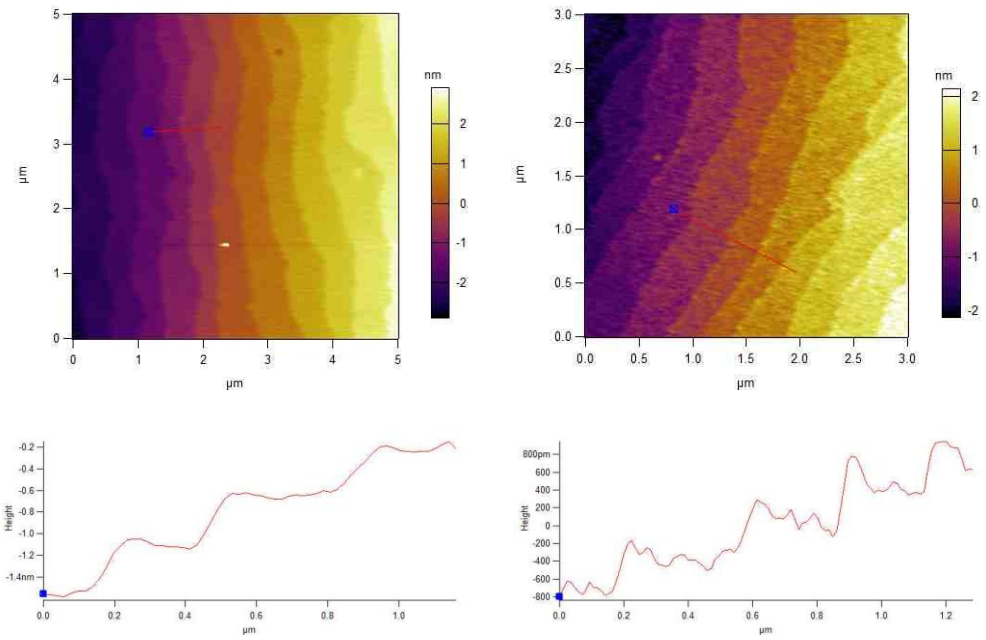

Figure. 14| Atomic force microscopy image and step height- width graph for (Left) SRO surface and (Right) Nb:STO surface.

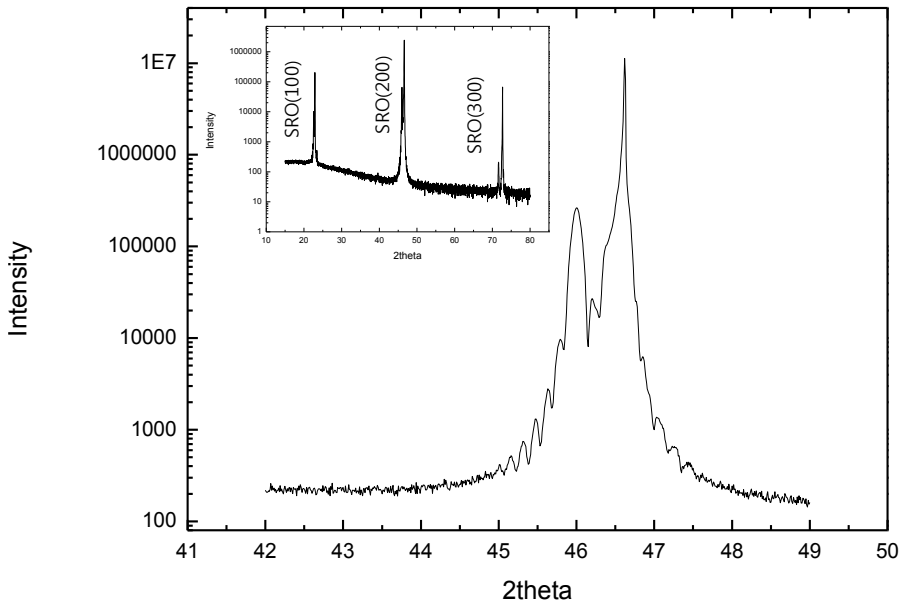

Figure. 15| X-ray diffraction data for STO/SRO/STO junction. FWHM : 0.06

For this reason, device of SRO and STO thin film is appropriate to characterize the electrical properties and interface electronic structure in detail. Ti (50nm) was chosen as a bottom electrode and deposited on the STO in a size of 50 μm cell using photolithography and sputtering. Tantalum (50nm) and Aluminum (50nm) were further deposited on Ti to avoid the oxidation of Ti. While SRO has a deep work function, Ti has a lower work function to make the Ohmic contact with STO so that the electric behavior could be determined by the top electrode only.

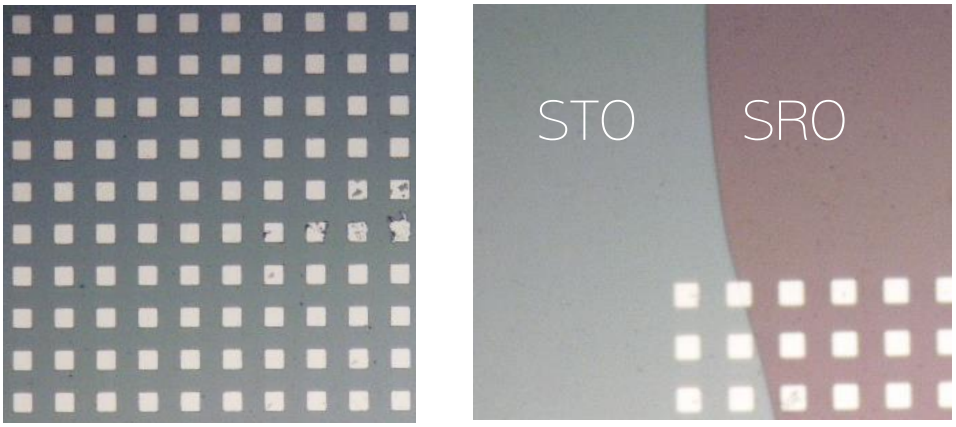

Figure. 16| Optical microscopy image of electrode patterning by photolithography and sputtering, Ti/Ta/Al (Left) and exposed SRO electrode by Ar ion etching

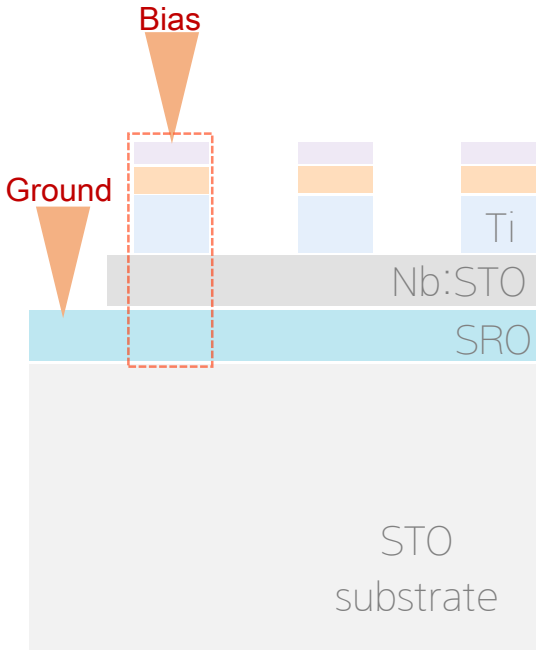

Figure. 17| Schematic of SRO/Nb:STO/Ti/Ta/Al ReRAM system

3.1.2. Electrical property measurement (I-V switching)

I-V measurements were performed using the Keithley 2400 semiconductor system, and reproducibility of each cell was confirmed. The negative bias was applied for switching to low resistance state (LRS) and the positive bias was applied for switching to high resistance state (HRS). The I-V hysteresis was probed by sweeping from 0V to 3.5V and from 0V to -4V. The same equipment was used to confirm the retention of each state, HRS and LRS, after certain hours with small read voltage 0.5V.

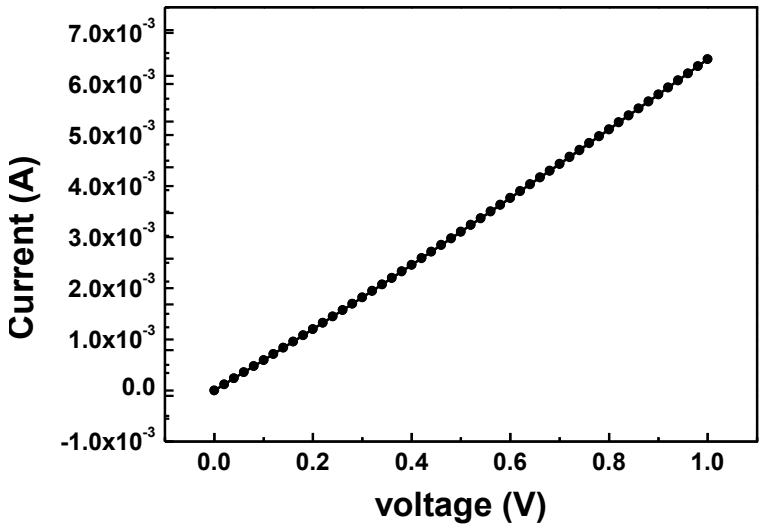

Figure. 18| Ti/STO/Ti Ohmic conduction I-V curve

3.1.3. TEM sample preparation

In this system, crossectional TEM specimen was prepared by focused ion beam (FIB) because the size of each cell is too small to make the specimen FIB can be used to select a specific area of interest in a sample, and besides FIB could produce as many TEM samples as possible in one device with confirming the reproducibility of switching behavior. Although TEM sample is easy to be damaged when it is milling under ion beam, modern FIB in low energy ion beam under 2kV can reduce a damage layer significantly.

Additionally, we always employed a Nanomill, focused low energy Ar ion miller from Fischion, for removing damage layer remained on surface of the specimen after FIB procedure. Because Nanomill uses ion beam under 1 kV, it is appropriate for fine milling step of FIB sample. We confirmed that the FIB sample specifically can become cleaner and thinner than before Nanomill procedure, and it is appropriate to acquire EELS.

This process for TEM specimen preparation, which is we conducted in this study, can be an optimal method for creating the high-quality thin specimen needed for advanced TEM analysis.

3.2. TEM experiment

3.2.1. Normal TEM

TEM is a microscopy technique in which a beam of electrons is transmitted through an ultra-thin specimen, interacting with the specimen as it passes through. An image is formed from the interaction of the electrons transmitted through the specimen, the image is magnified and focused to be detected by a sensor such as a CCD camera.

Most recently, advances aberration corrector design have been able to reduce spherical aberrations and to achieve resolution below 0.5Å at magnifications above 50 million times. Improved resolution allow for the imaging of lighter atoms that scatter electrons less efficiently. The ability to determine the position of atoms within materials has made the HRTEM an indispensable tool for nanotechnology research and development in many fields. High-resolution TEM is an imaging mode of the TEM that allows for direct imaging of the atomic structure of the sample. HRTEM is a powerful tool to study properties of materials on the atomic scale, and based on that, formations of the new layer or different phase can be elucidated in the vicinity of the interface.

In this study, analytical transmission electron microscopy (TEM) including high-resolution image, electron diffraction and scanning transmission electron microscopy (STEM)/electron-energy loss spectroscopy (EELS) was employed to elucidate the change at the interface.

3.2.2. *In-situ* STM/TEM (I-V switching)

We additionally confirmed the resistive switching and electrical property by *In-situ* scanning tunneling microscope/transmission electron microscope double tilt holder was employed to probe the current-voltage (I-V) measurement in the same environment of operating and observing the sample. The change of microstructure with electrical signal can be observed by *In-situ* observation, and besides, it can reduce other influence from the process of preparing TEM specimen in ex-situ experiment.

In-situ STM / TEM double tilt holder, Nanofactory, was employed to conduct the electrical switching and measurement. *In-situ* SET of RESET process both were conducted by STM tip was in contact with top electrode (Ti). In this system, voltage is biased to Cu grid, and the ground is on the tip, which is opposed to *ex-situ* switching system.

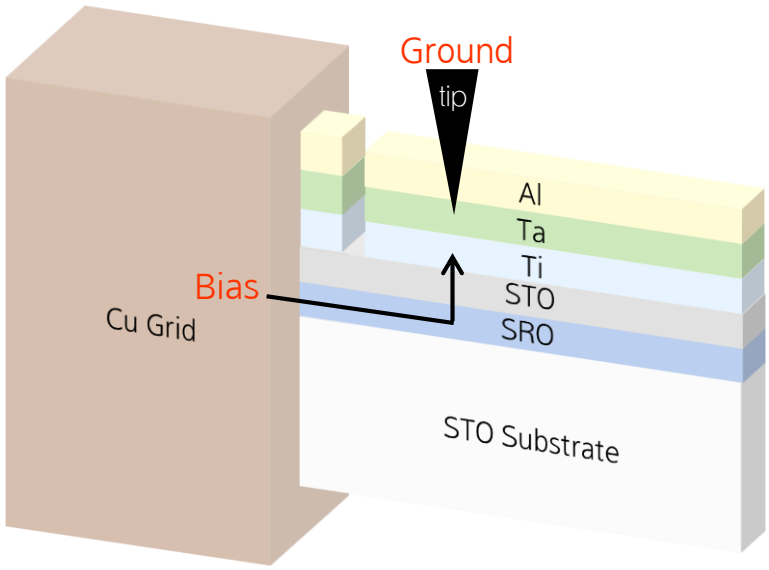

Figure. 19| Schematic diagram of the TEM sample for *In-situ* I-V experiment and I-V curve of *In-situ* switching

3.2.3. STEM-EELS

A scanning transmission electron microscope (STEM) is a type of TEM. STEM is distinguished from TEM by focusing the electron beam into a narrow spot which is scanned over the sample. The rastering of the beam across the sample makes there microscopes suitable for analysis techniques such as mapping by energy dispersive X-ray spectroscopy (EDS), electron energy loss spectroscopy (EELS) and annular dark-field imaging (ADF). These signals can be obtained simultaneously, allowing direct correlation of image and quantitative data. By using a STEM and a high-angle annular dark field (HAADF) detector, it is possible to form atomic resolution images where the contrast is directly related to the atomic number (z-contrast image). The directly interpretable z-contrast image makes STEM imaging with a HAADF detector appealing. This is in contrast to the conventional HRTEM technique, which uses phase-contrast, and therefore produces results which need interpretation by simulation.[30]

EELS as a STEM measurement technique made possible with the addition of an electron spectrometer. The high-energy convergent electron beam in STEM provides local information of the sample, even down to atomic dimensions. With the addition of EELS, elemental identification is possible and even additional capabilities of determining electronic structure and chemical bonding of atomic columns. In EELS, a material is exposed to a beam of electrons with a known, narrow range of kinetic energies. Some of

the electrons will undergo inelastic scattering, which means that they lose energy and have their paths slightly and randomly deflected. The amount of energy loss can be measured via an electron spectrometer and interpreted in terms of what caused the energy loss. The low-angle inelastically scattered electrons used in EELS compliments the high-angle scattered electrons in ADF images by allowing bot signals to be acquired simultaneously.

EELS is spoken of as being complementary to EDS, which is another common spectroscopy technique available on many electron microscopes, EDS excels at identifying the atomic composition of a material, is quite easy to use, and is particularly sensitive to heavier elements. EELS has historically been a more difficult technique but is in principle capable of measuring atomic composition, chemical bonding, valence and conduction band electronic properties, surface properties, and element specific edges tend to be sharp, well-defined, and at experimentally accessible energy losses (the signal being very weak beyond about 3 keV energy loss). EELS is perhaps best developed for the elements ranging from carbon through the 3d transition metals. The spectra of 3d transition metals can be analyzed to identify the oxidation states of the atoms. This ability to "fingerprint" different forms of the same element is a strong advantage of EELS over EDS. The difference is mainly due to the difference in energy resolution between the two techniques (~1 eV or better for EELS, perhaps a fer times ten eV for EDS).[31]

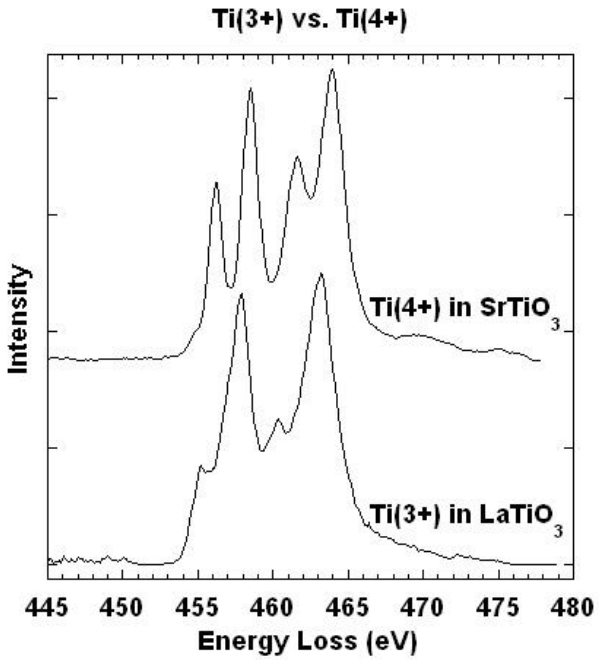

Figure. 20| Reference EELS spectra of Titanium. Microscope: FEI Tecnai T20, Energy Resolution: 0.45eV. [32]

4. Result of experiment

4.1. Electrical property

4.1.1. I-V measurement and Resistance change

We confirmed the resistive switching in all of the cells through the I-V curve. Since the interface between STO and Ti has the Ohmic contact, the resistive switching may occur at the SRO/STO interface. The LRS sample investigated in this work was prepared by applying negative bias (0→ -4 →0V), and the HRS sample by applying positive bias (0→ +3 →0V).

During the I-V measurements, switching occurred after extra forming process (-4.2V) which is often required in the filamentary conduction system, indicating that the entire interfacial area was not active for switching at first. As well as the on/off ratio (HRS/LRS ratio) was almost 10 at the read voltage (0.5V), the difference of resistance change increased between 1V and 3V. However, the sample was broken above 5V, the switching experiment was carefully conducted for the compliance current and the voltage.

The junction of SRO and STO was expected to not show resistive switching characteristics, because it has been known that STO without doping only show rectifying characteristics not resistive switching.[11] However, we observed the resistive switching phenomenon in the system of SRO/STO/Ti after forming process, and the observed I-V curve shows that there are Schottky barrier at this junction. Resistive switching appears only when rectifying characteristic appears in the junction of STO and metal electrode.

Therefore, the rectifying I-V curves in this system may be caused by the potential barrier at the interface of SRO/STO.[11,24]

4.1.2. Retention

A data retention time, the resistance state is maintained, of > 10 years is required for universal non-volatile memory. This retention time must be kept at thermal stress and small electrical stress such as a constant stream of read voltage pulses. Besides, it is crucial to know how long the resistance states are maintained for the TEM experiment which needs a long time for preparing the TEM specimen.

Retention time was confirmed in two different ways, one of them is to measure the particular resistance state after a certain period time and the other one is successional measurement of the resistance.

First of all, each of cells switched to HRS and LRS was measured its resistance state again after a certain time. Measuring voltage was +0.5V for HRS and -0.5V for LRS. The I-V curves obtained from the cells after specific time are as follows. Many cells were confirmed that resistance state was maintained for a long time. However, a few of them did not retain their resistance state, which means the resistance state seemed to gradually increase for LRS of decrease for HRS. Therefore, we identified the retention using the second way.

For the second way, we confirmed the each state through the initial current just the same way for the first. The read voltage was the small opposite bias for each state, +0.2V for LRS and -0.2V for HRS, to confirm whether the resistive switching occurs with the time dependence for a small voltage. And besides, although we considered that the read voltage (-0.2V) continuously

affected the cell state causing the movement of ions or electrons, the current did not increase or decrease for each of the HRS and LRS samples as the continuous measurement. However, there is a weakness in this way, which is difficult to measure the resistance state for a long time in this way.

For TEM analysis, it is crucial to keep the resistance state at the time to observe the sample, because it takes a lot of time for preparing the TEM specimen as well as analysis time. Therefore, we confirmed the resistance state of the cell for each steps, after FIB sampling, Nanomill, and TEM analysis. This process support the TEM observation was conducted in confirmed resistance states.

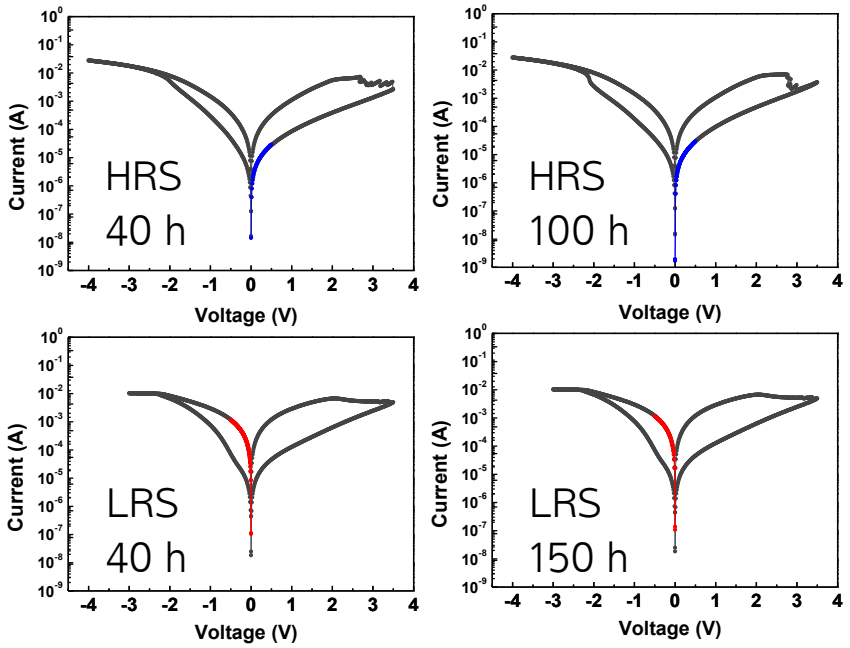

Figure. 21| Retention confirmation after specific time for each state of HRS (top) and LRS (bottom). Read voltage 0.5V for HRS (blue line) and -0.5V for LRS (red line)

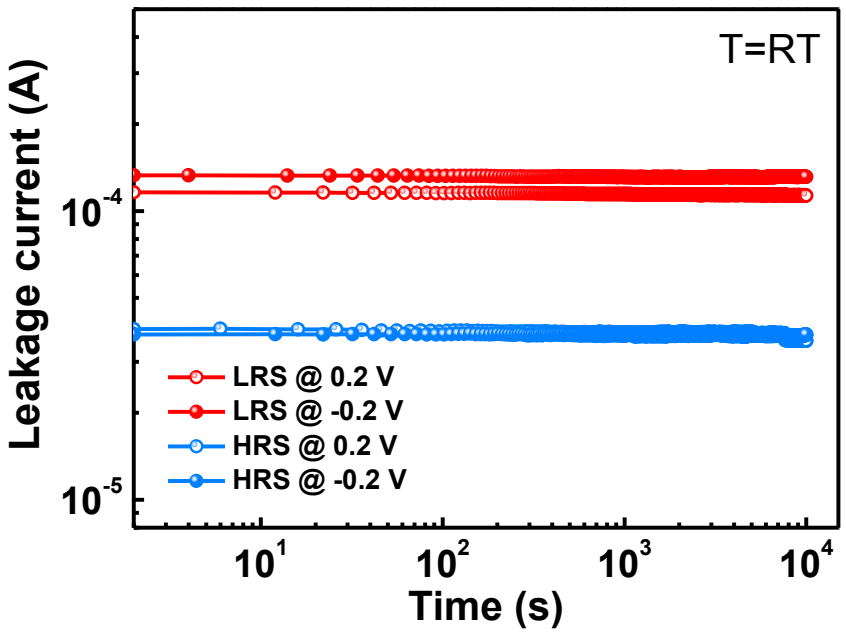

Figure. 22| Continuous resistance measurement for LRS (red) and HRS (blue). Read voltage +0.2V for LRS and -0.2V for HRS.

4.2. Investigation of the reason for resistance change behavior by TEM investigation

4.2.1. High resolution image of each resistance state

We analyzed the each specimen for HRS and LRS by HR-TEM imaging and STEM imaging and we cannot figure out the difference between HRS and LRS, chemical reaction layer or formation a new structure.

In other words, we cannot distinguish between two resistance states for imaging, and thus, we conducted STEM-EELS analysis in sequence.

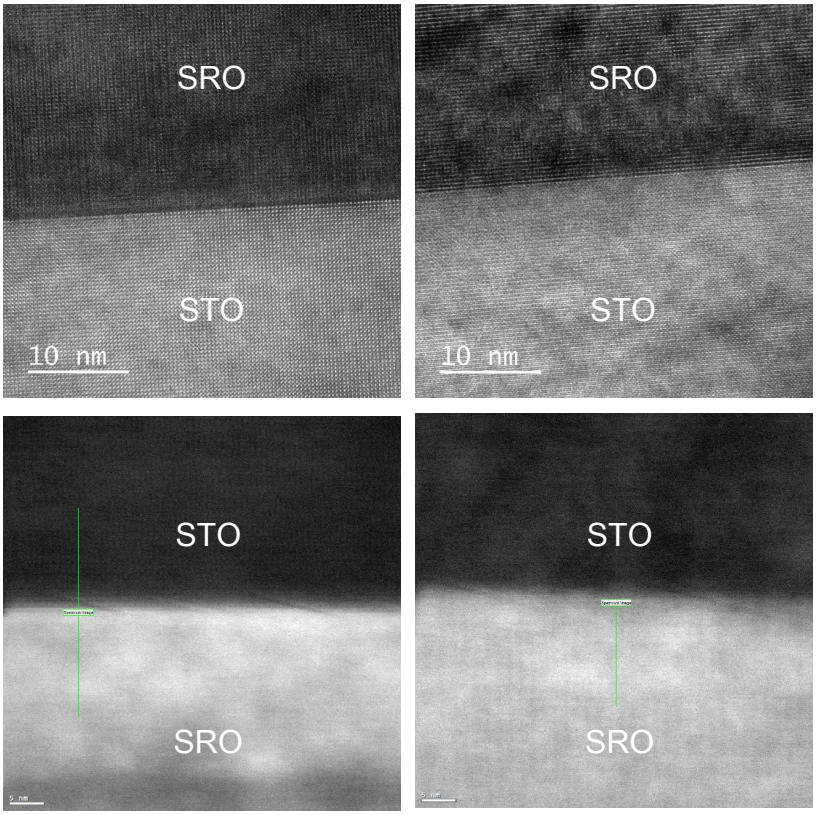

Figure. 23| HR-TEM, STEM image for LRS (left) and HRS (right).

4.2.2. STEM-EELS analysis of each resistance state

We confirmed each electronic structure of HRS and LRS in the vicinity of interface. At first, it is anticipated to exist the difference between HRS and LRS at a few nm areas, and thus the experiments were conducted for high resolution. Furthermore, EELS experiment using line profile across the SRO/STO interface was conducted for unraveling the difference between interface and bulk area.

In high-resolution STEM-image, we cannot find any difference between HRS and LRS samples. Besides, the EELS results also did not show any difference at the Ti L-edge and O K-edge spectrum, which means the concentration of oxygen vacancies does not cause the resistive switching in this system.

Generally, orbital splitting at the Ti L-edge, L_2 and L_3 peaks, does not occur in STO containing a lot of oxygen vacancies, which means the valence state of Ti changes from Ti^{4+} to Ti^{3+}. On the other hand, in the case of STO containing a few oxygen vacancies, we can observe the relatively clear L_2, L_3 peaks. In this case, Ti^{4+} valence state is maintained because most of oxygen is combined in STO. Similarly, O K-edge fine structure is sensitive to O-O ordering, and damps out as the vacancy concentration increases. EEL-spectrum obtained from this experiment, does not show the change of oxygen vacancies concentration in the vicinity of the interface. Considering that many researchers have suggested that the movement of oxygen vacancies results in

the resistive switching in the junction of oxide and metal electrode, this result can be astonishing finding.

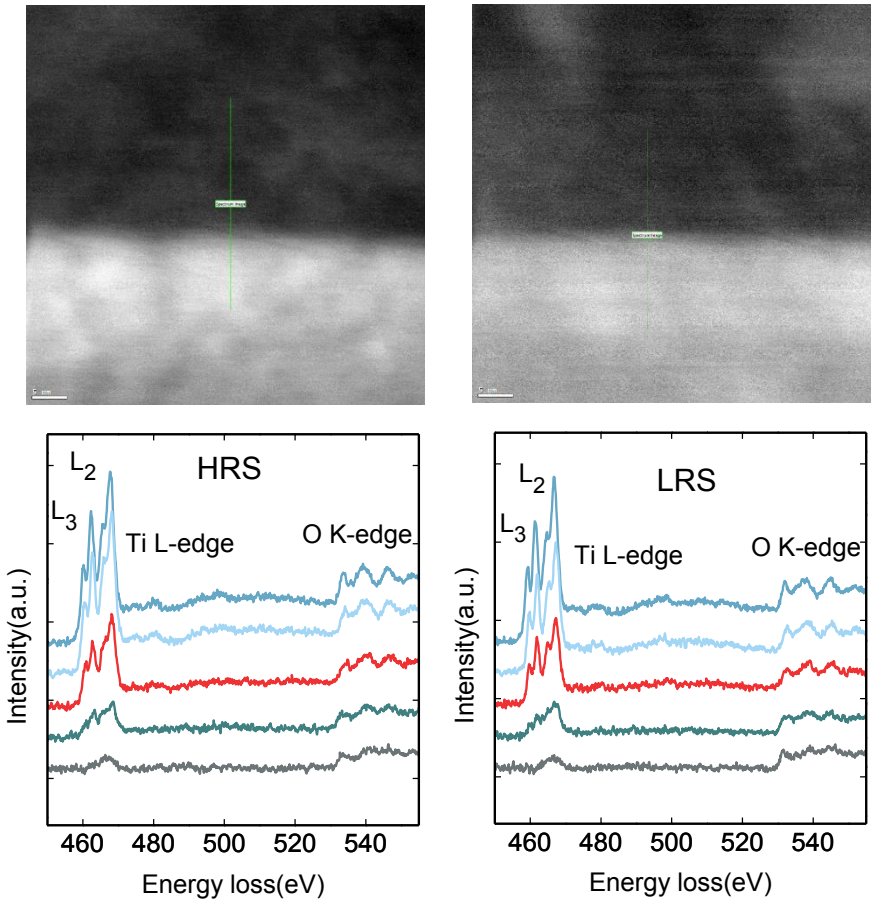

Figure. 24| STEM-EELS line profile. (Left) STEM-image and Ti L-edge, O K-edge EELS line profiles of HRS interface. (Right) STEM-image and EELS line profiles of LRS interface.

4.3 Unraveling the reason of resistance change in SRO/STO system

According to the previous research results, oxygen vacancy concentration is the main factor to determine the resistance of the device. However, in this experiment, oxygen vacancy concentration does not show any difference between high resistance state and low resistance state. This results can be interpreted for two conclusions.

At first, the difference of oxygen vacancy concentration between HRS and LRS may not have been detected due to the specification limit of EELS detector. In other ways, the absolute minuscule quantities of oxygen vacancy could not have been distinguished. Considering the interface at SRO/STO junction is well defined, the overall oxygen vacancies can be reduced by the absence of interface layer. This explanation is supported by the results that the on/off ratio is relatively small in this system. Actually, although the origin of resistance change is the concentration of oxygen vacancies, if the difference cannot be found, we cannot conclude the cause of resistance switching is oxygen vacancy movement. Therefore, the additional experiments need to prove the disparity of oxygen vacancy. For example, H_2-annealed STO in which oxygen vacancies are intentionally increased and SRO junction will be appropriate sample for comparison. There is another way to prove oxygen vacancy concentration using the spatial resolution TEM or high-resolution EELS detector.

Second, another factor which influences the resistance change of the bipolar resistive switching device should be considered to unravel the switching mechanism in this system. For SRO/STO junction, oxygen vacancy and oxygen ion are commonly considered as origin of switching, however, the other factor can influence the switching behavior. In our experimental results, there is no distinction between HRS and LRS, which can underpin the existence of another factor. Thus, microstructural analysis should be conducted not focusing on the oxygen vacancy. For instance, calculation of the interface trap density using the conductance loss or the equivalent parallel conductance loss measurement is required to find any difference between each resistance state.

5. Conclusion

We have studied the bipolar resistive switching mechanism for the transition metal oxide of perovskite structure. In previous studies, various types of homogeneous bipolar switching mechanism have been proposed, and most of them explain the switching behavior resulted from change of the potential barrier by electrochemical ion migration or charge trap/detrap. However, these suggestions are not enough to prove the mechanism for microstructural observation at the interface, and besides, there is no explanation about the bipolar resistive switching in the SRO/STO system.

Here, we investigated the SRO and STO single crystal junction device as the most ideal homogeneous bipolar resistive switching model system for TEM experiment. We confirmed the bipolar resistive switching and electrical property by I-V curve and measured the retention of the cell. Atomic distribution and electronic structure in the vicinity of the interface were investigated for each resistance state, however, we cannot detect the difference of oxygen vacancies distribution between HRS and LRS. This experimental results can be concluded for two ways. First, the amount of oxygen vacancies is too small to detect in this well-define interface system, additional experiments for unravelling the origin of resistive switching should be conducted like for SRO/H_2-annealed STO system. Second, other factors such as interface trap density will be considered using capacitance loss measurement except for oxygen vacancy concentration. This research could

not have revealed the exact origin of resistive switching, however, through these experimental results, we can know that it is important to take account of another factor for establishing the bipolar resistive switching mechanism not oxygen vacancy, and besides, this result may be helpful to do an additional experiment.

Reference

[1] Fujii, T., et al. Physical review B 75(16): 165101. (2007).

[2] Matt Marinella, 8th Annual Full Day Symposium Energing Non-Volatile Memory Technologies, (2012)

[3] P.H. Nielsen and N.M. Bashara., et al. *IEEE Transactions on Electron Devices*, Vol 11, P.243.(1964)

[4] J. G. Simmons and R. R. Verderber, et al., Proc. R. Soc. A., vol. 301, pp. 77–102, (1967)

[5] C. J. Varker and E. M. Juleff "Electron beam recording in SiO2 with direct read-out using the electron beam induced current at a p-n junction" Proceedings of IEEE, vol. 55, no. 5,pp. 728–729, (1967)

[6] D. J. Wouters "Oxide Resistive RAM (OxRRAM) for scaled NVM application" IMST 2009 Tutorial 9 Sept, (2009)

[7] W. W. Zhuang., et al. Tech. Dig. International Electron Devices Meeting, San Francisco, CA, pp. 193–196. (2002)

[8] I. G. Baek, et al. in Tech. Dig. Int. Electron Devices Meeting., San Francisco, CA, pp. 587–590. (2004)

[10] R. Waser, et al. Advanced Materials, 21, page 2632. (2009)

[11] Sawa, A., et al. "Resistive switching in transition metal oxides." Materials today 11(6): 28-36. (2008)

[12] Kwon, D.-H., et al. Nature nanotechnology 5(2): 148-153.(2010)

[13] Lee, S., et al. (2014). APL Materials **2**(6): 066103. (2014)

[14] Sim. H., et al., Tech. Dig. IEDM , 758 (2005)

[15] Warren, W. L., et al. Journal of the American Ceramic Society 79(2): 536-538 (1996).

[16] Leisegang, T., et al. Physical review letters 102(8): 087601 (2009)

[17] Strukov, D. B., et al. small 5(9): 1058-1063. (2009)

[18] Strukov, D. B., et al. nature 453(7191): 80-83 (2008).

[19] Tsui, S., et al., Appl. Phys. Lett. 85, 317 (2004)

[20] Seong, D.-J., et al., Electrochem. Solid-State Lett. 10, H168 (2007)

[21] C. Park., et al. J. Appl. Phys. 103, 054106 (2008)

[22] M. Kareev., et al. Appl. Phys. Lett. 93, 061909 (2008)

[23] N. Shanthi and D. D. Sarma, Phys. Rev. B 57, 2153 (1998))

[24] Sawa, A., et al. Applied Physics Letters 85(18): 4073-4075.) (2004).

[25] S.M.Sze, Physics of Semiconductor Devices, 2nd ed. Wiley, New York, (1981)

[26] Y. Tokura., et al. Phys. Rev. Lett. 70, 2126 (1993)

[27] K. van Benthem., et al. C. Elsässer and R. H. French Journal of Applied Physics 90: 6156. doi:10.1063/1.1415766. (2001).

[28] C.B.Eom, R.J.Cava, R.M.Leming, J.M.Phillips, R.B.van Dover, J.H. Marshall, J.W.P.Hsu, J.J.Krajewski, and W.F.Peck Ju., Science 258, 1766 (1992)

[29] N.Nakagawa, H.T.Hawng, and D.A. Muller, Nature Mat. 5, 204 (2006)

[30] http://muller.research.engineering.cornell.edu/sites/WEELS/

[31]https://en.wikipedia.org/wiki/Scanning_transmission_electron_microscopy

[32] https://en.wikipedia.org/wiki/Electron_energy_loss_spectroscopy

국문 초록

끊임없이 변화하는 IT 환경 속에서, 전자 제품의 급속한 성능 향상을 위해 저장매체에도 고용량, 고성능, 저전력 동작 등 다양한 변화들이 요구되고 있다. 현재 대표적인 메모리인 DRAM 이나 Flash 메모리 같은 고집적 메모리 기술은 지속적인 scaling down 으로 공정 난이도가 증가되었고, 더 이상의 미세화가 어려워지면서 기술적인 한계가 초래되었다. 따라서 이러한 물리적, 기술적 한계를 극복하기 위해 새로운 저장 매체 기술에 대한 연구가 활발히 진행되고 있는데, 차세대 메모리 후보 군 중 하나인 저항변화메모리(ReRAM)는 빠른 스위칭 속도, 낮은 구동전압, 간단한 소자 구조를 갖는 등 여러 가지 장점을 가진다.

ReRAM 은 금속/부도체/금속의 구조로 이루어져있으며, 외부에서 가해지는 전기적 자극에 의해 저항의 변화가 일어나게 되고, 이를 메모리 신호인 0 과 1 로 사용한다. ReRAM 은 작용 특성에 따라 크게 두 가지로 구분이 가능한데, 소자의 저항이 가해준 전기적 자극의 크기에 따라서 변하는 특성을 단극성 (unipolar) 저항변화, 전기적 자극의 극성에 따라서 변화는 특성을 양극성 (bipolar) 저항변화라 한다. 단극성 저항변화 소자의 경우, 어떠한 극성의 전압을 가해주더라도 하나의 극성에서 저항이 낮아지고 높아지는 현상이 모두 일어난다. 대부분의 소자에서 단극성 저항변화의 경우 전도성 영역인 필라멘트의 형성과 소멸로

인하여 저항이 변화한다고 알려져 있다. 반면, 양극성 저항변화 소자의 경우에는 저항이 낮아지고 높아지는 현상이 서로 다른 전압의 극성에서만 이루어질 수 있는데, 소자의 구조나 종류에 따라서 여러 가지 특징을 나타내기 때문에 여전히 메커니즘의 규명이 이루어지지 않고 이러한 현상을 설명하는 다양한 주장들이 존재한다. 양극성 저항변화 소자에서 균일한 저항변화 현상이 일어나는 경우, 주로 계면에서의 변화를 원인으로 꼽는다. 이 모델에서는 계면의 미세 구조 변화가 저항변화 현상을 결정하는 중요한 요인이 되지만, 직접적으로 계면을 관찰하는 것은 매우 어려우므로, 이를 통해 증명해낸 연구 결과가 부족한 실정이다.

이 연구에서는 양극성 저항변화 특성을 갖는 $SrRuO_3$3/$SrTiO_3$ 접합 소자에서 메커니즘을 규명하기 위해 투과전자현미경을 이용한 실험을 진행하였다. SRO 는 STO 와 매우 유사한 격자상수 값을 가질 뿐만 아니라, 화학적으로도 매우 안정하다고 알려져 있다. 뿐만 아니라, oxide 간의 접합이기 때문에, 저항 변화 원인으로 많은 주목을 받는 oxygen vacancy 나 oxygen ion 의 이동이 매우 용이할 것으로 여겨지기 때문에, 양극성 저항변화 현상의 원인 및 메커니즘을 규명하기 위한 매우 적합한 소자라고 생각되었다. I-V 의 측정 및 분석을 통해 저항변화 현상과 전기적 특성을 측정하였으며, 저항 상태에 따른 소자에서 TEM

분석 및 STEM-EELS 분석을 진행하였다. 그리고 in-situ STM/TEM holder 를 이용하여, TEM 내에서 소자의 전기적 특성을 측정하고 소자가 거동하는 환경에서 직접적인 변화를 살펴보았다. 계면에서 저항변화 현상을 설명하는 데에 중요한 요인으로 생각되는 oxygen vacancy 의 변화는 이 실험 내에서 관찰되지 않았다. 이러한 실험 결과는 두 가지로 해석될 수 있다. 우선 매우 잘 정의된 계면을 갖는 SRO/STO 소자에서는 계면이 매우 균일하므로, chemical reaction 등에 의해 생겨날 수 있는 oxygen vacancy 의 양이 줄어들게 되고, 이로 인해 저항변화 현상에 참여하는 절대적인 oxygen vacancy 의 양의 감소로 인해, 극 소량의 oxygen vacancy 의 변화가 측정되지 않았을 수 있다. 추가적으로 H_2 분위기에서 annealing 을 통해 STO 를 인위적으로 oxygen vacancy 의 양을 늘려주어 분석을 진행한다면, 상대적으로 많은 양의 oxygen vacancy 이동이 일어날 것이므로, 관찰이 용이할 수 있을 것이라 생각된다. 다음으로, oxygen vacancy 가 저항변화 현상의 원인이 아닐 것이라는 결론을 내릴 수 있다. 즉, Oxygen vacancy 이 외의 또 다른 trap site 존재가 저항변화 현상의 원인이 되어 EELS spectrum 에서는 분석이 불가능하였을 수 있다. 이는 SRO/STO system 에서 oxygen vacancy 나 oxygen ion 이 많이 존재함에도 불구하고, 저항이 높고 낮은 상태에서 oxygen vacancy 의 발견이 이루어지지 않은 실험 결과가 뒷받침할 수 있는 결론이다. 이는

interface 에 존재할 수 있는 trap site 의 정도를 측정하고 분석할 수 있는 방법을 통해 규명할 수 있을 것이라 생각한다.

본 연구를 통해 잘 정의된 계면에서 저항 변화 현상을 관찰하였을 뿐만 아니라 이 후에 양극성 저항변화 소자의 특성 및 메커니즘을 규명하는 데에 있어, 또 다른 요인을 생각해볼 수 있으며, 새로운 메커니즘을 정립하는 데에 큰 도움을 줄 수 있을 것이라 기대된다.

주요어 : 저항변화메모리, 양극성 저항변화, $SrTiO_3$, $SrRuO_3$, 투과전자현미경, 전자에너지손실 스펙트럼

학번 : 2013-23045